VUV photo-absorption spectroscopy of vinyl chloride studied by high resolution synchrotron radiation

ARTICLE *in* CHEMICAL PHYSICS · NOVEMBER 2006

Impact Factor: 1.65 · DOI: 10.1016/j.chemphys.2006.08.021

5 AUTHORS, INCLUDING:

Paulo Manuel Limão-Vieira
New University of Lisbon
178 PUBLICATIONS **1,482** CITATIONS
SEE PROFILE

Sekhar B.N.Raja
Raja Ramanna Centre for Advanced Techno…
65 PUBLICATIONS **166** CITATIONS
SEE PROFILE

N. J. Mason
The Open University (UK)
397 PUBLICATIONS **3,929** CITATIONS
SEE PROFILE

Available online at www.sciencedirect.com
ScienceDirect
Chemical Physics 330 (2006) 265–274
Chemical Physics
www.elsevier.com/locate/chemphys

VUV photo-absorption spectroscopy of vinyl chloride studied by high resolution synchrotron radiation

P. Limão-Vieira [a,b,*], Eva Vasekova [a], B.N. Raja Sekhar [c], N.J. Mason [a], S.V. Hoffmann [d]

[a] Laboratório de Colisões Atómicas e Moleculares, Departamento de Física, CEFITEC, FCT-Universidade Nova de Lisboa, 2829-516 Caparica, Portugal
[b] Department of Physics and Astronomy, The Open University, Walton Hall, Milton Keynes MK7 6AA, UK
[c] BARC-Spectroscopy Laboratory, Centre for Advanced Technology (CAT), Indore 452 013, India
[d] Institute of Storage Ring Facilities, University of Aarhus, Denmark

Received 19 May 2006; accepted 24 August 2006
Available online 30 August 2006

Abstract

The electronic state spectroscopy of vinyl chloride, C_2H_3Cl, has been investigated by high resolution VUV photo-absorption spectroscopy in the wavelength range 115–300 nm (10.8–4.2 eV). New assignments are proposed for Rydberg series converging to the four lowest ionisation energies and their associated vibrational excitation is observed for the first time. Absolute cross-section values have been obtained allowing photolysis lifetimes to be derived in the Earth's troposphere and stratosphere.

Keywords: Photo-absorption; Synchrotron radiation; Electronic and vibrational excitation; Rydberg series; Local lifetimes

1. Introduction

Small hydrocarbons and their halogenated derivatives play a significant role in many fields of physics, chemistry and biomedical sciences. As a part of a larger project, in which we investigate properties of gases with significance for the plasma etching industry [1] and evaluate their role in global warming in the Earth's atmosphere [2], we have recorded a high resolution VUV photo-absorption spectra of vinyl chloride. Vinylchloride, C_2H_3Cl, also known as chloroethene, chloroethylene, ethylene monochloride, or monochloroethylene, is a colourless gas at STP. It is an anthropogenic species either released directly into the atmosphere or formed from the breakdown of other anthropogenic substances, such as trichloroethene and tetrachloroethene. Most of the vinyl chloride produced is used to make polyvinyl chloride (PVC).

The first absorption spectrum in the 5.4–12.4 eV energy region was reported by Walsh [3] and a UV photo-absorption spectrum in the 6.2–11.5 eV region has been published by Sood and Watanabe [4] using a H_2 discharge tube. Brion and co-workers have reported He(I) and He(II) photoelectron spectra of monohaloethylenes and studied valence shell excitation using electron energy loss spectroscopy under pseudo-optical conditions at an incident electron energy of 3 keV [5]. More recently Locht et al. [6] reported the photo-absorption spectrum of vinylchloride in the 8–12 eV energy range identifying and classifying several valence and Rydberg transitions. However, they only reported relative photo-absorption cross-section values. Most recently Arulmozhiraja et al. [7] explored the photodissociation mechanisms of vinylchloride using of symmetry-adapted cluster configuration interaction (SAC-CI) theory to determine vertical excitation energies.

2. Experimental

The present high resolution VUV photo-absorption measurements were performed on the ASTRID – UV1

* Corresponding author. Tel.: +351 21 294 85 76; fax: +351 21 294 85 49.
E-mail address: plimaovieira@fct.unl.pt (P. Limão-Vieira).

0301-0104/$ - see front matter © 2006 Published by Elsevier B.V.
doi:10.1016/j.chemphys.2006.08.021

beam line at the Institute for Storage Ring Facilities (ISA), University of Aarhus, Denmark. A detailed description of the apparatus can be found elsewhere [8] so only a brief description will be given here. A toroidal dispersion grating is used to select the synchrotron radiation with a FWHM wavelength resolution of approximately 0.075 nm. The synchrotron radiation passes through the gas sample stored in a gas cell maintained at room temperature. A photo-multiplier is used to detect the transmitted light. For wavelengths below 200 nm a flow of He gas is flushed through the small gap between the photomultiplier and the exit window of the gas cell to prevent any absorption by air contributing to the spectrum. The LiF entrance window acts as an edge filter for higher order radiation restricting the photo-absorption measures to below 10.8 eV (115 nm). The grating itself provides a maximum wavelength (lower energy limit) of 320 nm (3.9 eV). The sample pressure is measured by a Baratron capacitance gauge. To avoid any saturation effects sample pressures were chosen such that the transmitted flux was >90% of the incident flux. The synchrotron beam ring current is monitored throughout the collection of each spectrum to allow for normalisation of the incident flux. Results are compared to a background scan recorded with an evacuated cell. Absolute photo-absorption cross-sections may then be calculated using the Beer–Lambert law:

$$I_t = I_0 \exp(-n\sigma x),$$

where I_t is the intensity of the light transmitted through the gas sample, I_0 is that through the evacuated cell, n is the molecular number density of the sample gas, σ is the absolute photo-absorption cross-section and x is the absorption path length (25 cm).

The samples of vinyl chloride were purchased from Sigma–Aldrich, with a stated purity >99.5%, no further purification was performed.

3. Results

3.1. Spectroscopy of vinyl chloride

In its ground state vinyl chloride has C_S symmetry, with 12 vibrational modes [9]. In the present absorption spectrum only vibrational modes with excitation energies of 0.199, 0.159, 0.083 and 0.049 eV were observed. Comparing these values with vibrational energies of the ground state these may be assigned to the $\nu_4(a')$ excitation C=C stretching mode (with a CH_2 scissoring contribution), the $\nu_6(a')$ H–C–Cl scissoring mode, the $\nu_8(a')$ C–Cl symmetric stretching mode (with a CH_2 rocking contribution) and the $\nu_9(a')$ CH_2 in plane rocking. In the electronic ground state configuration of C_2H_3Cl the valence outermost orbitals are $(5a')^2\ (6a')^2\ (1a'')^2\ (7a')^2\ (2a'')^2$: $\tilde{X}^1A'$. The highest occupied molecular orbital (HOMO) has π_{CC} character ($2a''$) followed at higher binding energies by $n_{p\|}$(Cl) ($7a'$), $n_{p\perp}$(Cl) ($1a''$) and σ_{C-Cl} ($6a'$). The lowest unoccupied molecular orbitals are the virtual valence σ^*(C–Cl) and π^*(CC). The major absorption bands in the measured VUV photo-absorption spectrum can be ascribed to excitations from these HOMOs to the LUMOs followed by several Rydberg series converging to the first, second and third ionic excited states (Fig. 1). The four lowest vertical ionisation energies of C_2H_3Cl obtained by Brion and co-workers for the $(2a'')^{-1}$, $(7a')^{-1}$, $(1a'')^{-1}$ and $(6a')^{-1}$ orbitals, are 10.16, 11.64, 13.10 and 13.60 eV, respectively [5].

The members of any Rydberg series with energy E_n must fit the Rydberg formula: $E_n = E_i - R/(n-\delta)^2$, where E_i is the ionisation energy, n is the principal quantum number of the Rydberg orbital of energy E_n, R is one Rydberg and δ the quantum defect resulting from the penetration of the Rydberg orbital into the core. It should be noted that Rydberg series may be associated with either the carbon atoms or the chlorine atoms. Due to the lower resolu-

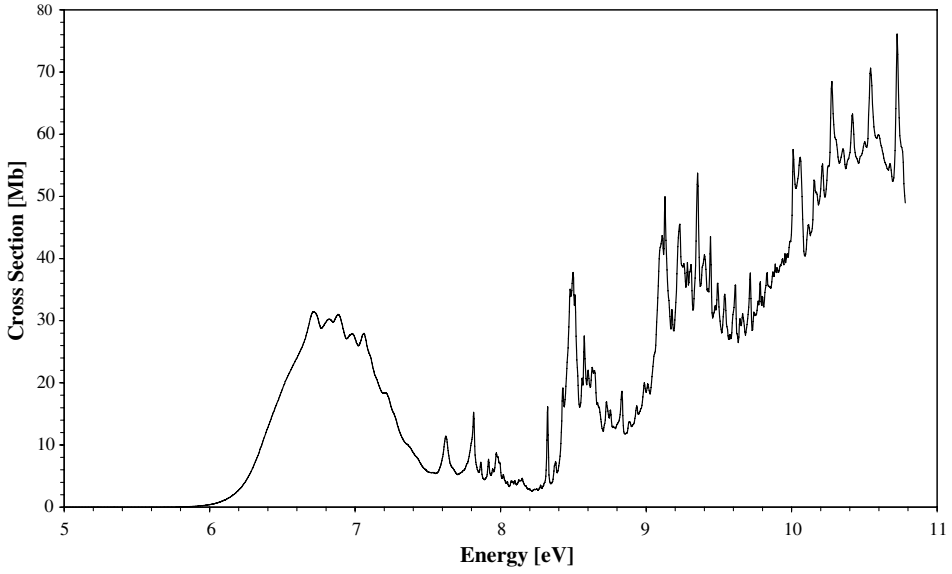

Fig. 1. The VUV photo-absorption spectrum of C_2H_3Cl in the 5.0–11.0 eV energy region.

tion in previous experiments few vibrational states have been observed in the Rydberg region [6], hence in the following discussion we present a detailed analysis of the vibronic structure observed and several new assignments are proposed (Tables 3–15). However, it should be pointed out that the normal mode description of vibrations is very powerful for the lowest lying excitations and a close look at the assignments show that two different vibrational modes can actually have the same value with therefore the possibility of strong Fermi resonances.

Fig. 1 shows the complete photo-absorption spectrum of vinyl chloride between 5.0 and 10.8 eV. All features observed in the photo-absorption spectrum have been identified and assigned to vibronic Rydberg transitions. We will now discuss each part of this spectrum in turn assigning all the observed features.

3.2. Valence excitation in the energy range 6.0–7.5 eV

The lowest absorption band in vinyl chloride is shown in more detail in Fig. 2. This band is attributed to the excitation of a (2a″) electron to the π^*(CC) together with excitation of an *n*s Rydberg orbital predominately attributed to the carbon atoms (see below) [7]. The $\pi^*_{CC} \leftarrow \pi_{CC}(2a'')$ band has a local maximum of 31.460 Mb at 6.709 eV, in good agreement with the 6.684 eV value reported by Brion et al. [5]. The weaker $\pi(2a'') \rightarrow \pi^*(CC)$ band also shows evidence, in the low energy side, of a shoulder that as been assigned to the v_{00} transition at 6.365 eV, observed in the spectra of other chloroethylenes [10], and been assigned as the $\sigma^*_{CCl} \leftarrow \pi_{CC}(2a'')$ transition. There is clear evidence of rich vibrational structure superimposed on the broad band (Table 1), this structure is shown here for the first time. Such structure appears to be associated also with the $3s : \widetilde{X}^2A'' \leftarrow 2a'' : \widetilde{X}^1A'$ Rydberg transition and the ν_4 C=C stretching mode (with a CH_2 scissoring contribution), the ν_8 C–Cl symmetric stretching mode (with a CH_2 rocking contribution) while the ν_9 CH_2 in plane rocking mode, also shows a long progression. In Table 2 we make use of the calculated values from Ref. [7] to compare with the present experimental transition energies of C_2H_3Cl.

Table 1
Energy positions and vibrational analysis of features observed in the first absorption band (6.0–7.5 eV) of C_2H_3Cl (energies in eV)

This work				
Energy	Assignment	$\Delta E(v'_4)$	$\Delta E(v'_8)$	$\Delta E(v'_9)$
6.365	v_{00}	–	–	–
6.464 (s)	$1\nu_8$	–	0.099	–
6.543	$1\nu_4$	0.178	–	–
6.641	$1\nu_4 + 1\nu_8$	–	0.098	–
6.709	$2\nu_4$	0.166	–	–
6.746 (s)	$2\nu_4 + 1\nu_9$	–	–	0.037
6.818	$2\nu_4 + 1\nu_8$	–	0.109	–
6.882	$3\nu_4$	0.173	–	–
6.919	$2\nu_4 + 2\nu_8$	0.101	–	
	$3\nu_4 + 1\nu_9$	–	0.037	
6.981	$3\nu_4 + 1\nu_8$	–	0.099	–
7.061	$4\nu_4$	0.179	–	–
7.099	$4\nu_4 + 1\nu_9$	–	–	0.038
7.136 (d)	$4\nu_4 + 2\nu_9$	–	–	0.037
7.163 (s)	$4\nu_4 + 1\nu_8$	–	0.102	–
7.202	$4\nu_4 + 1\nu_8 + 1\nu_9$	–	–	0.039
7.223 (b)	$5\nu_4$	0.162	–	–
7.265	$5\nu_4 + 1\nu_9$	–	–	0.042
7.326 (d)	$5\nu_4 + 1\nu_8$	–	0.103	–
7.380 (d)	$6\nu_4$	0.157	–	–
7.424 (d)	$6\nu_4 + 1\nu_9$	–	–	0.044
7.478 (d)	$6\nu_4 + 1\nu_8$	–	0.098	–

(s) means shoulder; (d) means diffuse structure; (b) means broad structure.

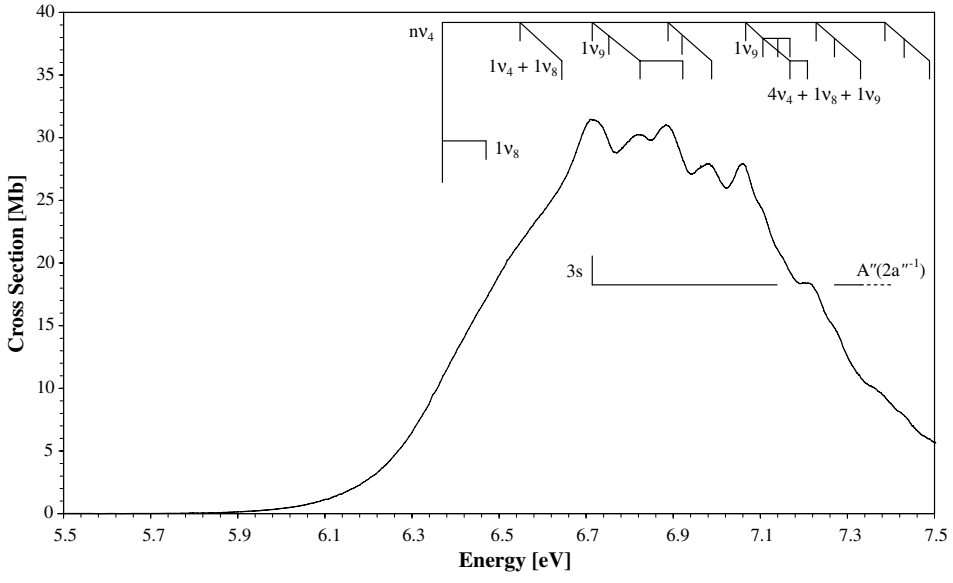

Fig. 2. The C_2H_3Cl photo-absorption spectrum from 5.5 to 7.5 eV with labelled vibrational series.

Table 2
Measured experimental transition energies in C_2H_3Cl compared to the calculated values from Ref. [7]

State	SAC-CI [7]			This work		Sze et al. [5]
	Nature	ΔE (eV)	Osc. strength, f	Cross-section (Mb)	Energy (eV)	Nature
$1^1A'$	Ground state	–	–	–	–	–
$1^1A''$	π–3s/σ^*_{C-Cl}	6.81	0.0111	10.485	6.365	σ^*_{C-Cl}
$2^1A'$	π–π^*	6.96	0.3274	31.460	6.709	π^*_{CC}
$2^1A''$	π–σ^*_{C-Cl}/3s	6.99	0.0035	–	–	–
$3^1A''$	π–3pσ_x	7.48	0.0006	–	–	–
$4^1A''$	π–3pσ_y	7.70	0.0102	11.407	7.623	σ^*_{C-Cl}
$5^1A''$	n_{Cl}–π^*	7.82	0.0005	–	–	–
$3^1A'$	π–3pπ	7.89	0.0098	15.266	7.815	σ^*_{C-Cl}
$4^1A'$	n_{Cl}–σ^*_{C-Cl}	8.20	0.0012	–	–	–
$6^1A''$	π–3dσ/4s	8.42	0.0152	16.138	8.324	–
$7^1A''$	π–3dσ/4pσ_x	8.46	0.0001	–	–	–
$5^1A'$	π–3dπ/4pπ	8.57	0.0050	22.030	8.601	–
$6^1A'$	n_{Cl}–3s	8.60	0.0465	37.772	8.498	π^*_{CC}
–	–	–	–	53.718	9.354	σ^*_{C-Cl}
–	–	–	–	35.710	9.615	π^*_{CC}
–	–	–	–	37.673	9.717	σ^*_{C-Cl}
–	–	–	–	68.492	10.278	π^*_{CC}

Rydberg 3s, 3p and 3d orbitals are mainly attributed to carbons whereas 4s and 4p to chlorine [7].

3.3. Rydberg series

The cross-section above 6.5 eV consists of a series of sharp peaks assigned as s, p and d Rydberg states progressing up to the four lowest ionisation limits, 10.16, 11.64, 13.10 and 13.60 eV (Figs. 3 and 4, Tables 3–15).

3.3.1. Rydberg series converging to the lowest ionic ground state, $\widetilde{X}^2A''(2a''^{-1})$

The first term of a *n*s series is found to lie at 6.709 eV (Table 3, Fig. 2), with a quantum defect $\delta = 1.01$ and corresponds to the $3s : \widetilde{X}^2A'' \leftarrow 2a'' : \widetilde{X}^1A'$ transition. The *n*s quantum defects for $n \geqslant 4$ are in good agreement with those reported by Locht et al. [6] and, in agreement with the SAC-CI calculations of Arulmozhiraja et al. (Table 3), are attributable to the carbon atoms [7]. The $n = 3$ peak position is hard to define due to the superposition of the peak with the ν_4 C=C stretching mode and the ν_9 CH_2 in plane rocking mode. The 4s term appears at 8.631 eV with a quantum defect of 1.02. The 9.991 eV peak assigned as $n = 10$ s has a quantum defect $\delta = 1.03$ slightly higher than expected which can be attributed to the fact that this peak is located on a shoulder structure.

The position of peaks attributed to the *n*pσ_y, *n*pπ, *n*dσ and *n*dπ series are shown in Fig. 3 and are listed in Tables 4–7, respectively. Once again the orbitals are associated with the carbon atoms. These values are compared with those calculated recently by Arulmozhiraja et al. [7], who

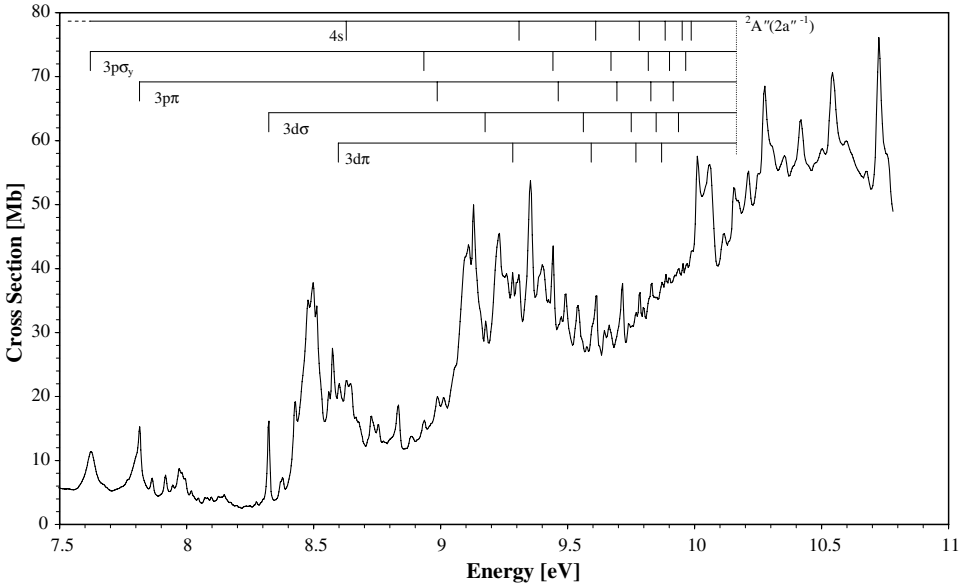

Fig. 3. The C_2H_3Cl photo-absorption spectrum from 7.5 to 11.0 eV with labelled Rydberg series converging to the ionic electronic ground state.

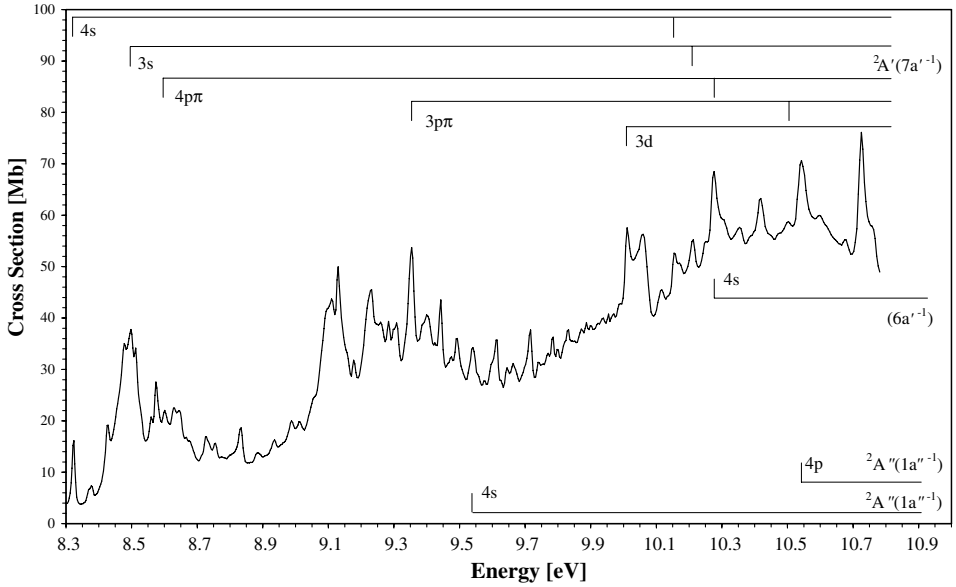

Fig. 4. The C_2H_3Cl photo-absorption spectrum from 8.3 to 11.0 eV with labelled Rydberg series converging to the first, second and third excited ionic states.

Table 3
Energy values, quantum defect and assignment of the vibrational excitation in *n*s (carbon) Rydberg series converging to the ionic ground state $\widetilde{X}^2A''(2a''^{-1})$ of C_2H_3Cl (energies in eV)

Energy	Quantum defect	Assignment	$\Delta E(v'_4)$	$\Delta E(v'_6)$	$\Delta E(v'_8)$	$\Delta E(v'_9)$
6.709	1.01	3s	–	–	–	–
8.631	1.02	4s	–	–	–	–
8.756	–	$4s + 1v_6$	0.125	–	–	
8.806 (s)	–	$4s + 1v_6 + 1v_9$	–	–	0.050	
8.885	–	$4s + 2v_6$	–	0.129	–	–
9.011	–	$4s + 3v_6$	–	0.126	–	–
9.308	1.00	5s	–	–	–	–
9.615	1.00	6s	–	–	–	–
9.717	–	$6s + 1v_8$	–	–	0.102	–
9.740	–	$6s + 1v_6$	–	0.125	–	–
9.786	0.97	7s	–	–	–	–
9.887	0.94	8s	–	–	–	–
9.954	0.88	9s	–	–	–	–
9.991 (s)	1.03	10s	–	–	–	–

(s) means shoulder.

also calculated the relative oscillator strengths (ROS) for each of these transitions. Comparison of these ROS with the strength of the feature observed in the measured spectrum provide another test of the assignment. The first terms of the $np\sigma_y$, $np\pi$, $nd\sigma$ series are found at 7.623, 7.815 and 8.324 eV, with quantum defects $\delta = 0.68$, 0.59 and 0.28, respectively. These energies are in good agreement with those reported by Robin [10] (7.628, 7.818 and 8.324 eV respectively). An extra Rydberg series of $nd\pi$ character, with its first term lying at 8.601 eV and a quantum defect $\delta = 0.05$, is observed for the first time.

3.3.2. Rydberg series converging to the ionic electronic first excited state, $\widetilde{A}^2A'(7a'^{-1})$

The first series (Table 8, Fig. 4) observed converging to the first ionic state with an ionisation energy of 11.64 eV [5] has been assigned to the chlorine lone pair electrons ($n_{Clp\|} \rightarrow ns$) lying at 8.324 eV with a quantum defect of $\delta = 1.98$. The first series attributed to the carbon atoms is a *n*s series with the first term being assigned to $n = 3$ at 8.498 eV, with quantum defects $\delta = 0.92$, in good agreement with the calculated values of Arulmozhiraja et al. [7] (see also Table 9).

The $np\pi$ series associated with the chlorine atom (Table 10, Fig. 4) has its first term at 8.601 eV the same peak position for the $nd\pi$ series converging to the electronic ionic ground state. A careful analysis of this peak reveals a non-symmetric shape that can be related to the superposition of these two series. The $n = 4$ member has a quantum defect of $\delta = 1.88$ and $n = 5$ peak at 10.276 eV has a $\delta = 1.84$.

The $np\pi$ series associated with the carbon atoms starting at 9.354 eV (Table 11), with $\delta = 0.56$ is mainly due to the

Table 4
Energy values, quantum defect and assignment of the vibrational excitation $np\sigma_y$ (carbon) Rydberg series converging to the ionic electronic ground state $\widetilde{X}^2A''(2a''^{-1})$ of C_2H_3Cl (energies in eV)

Energy	Quantum defect	Assignment	$\Delta E(v'_4)$	$\Delta E(v'_6)$	$\Delta E(v'_8)$	$\Delta E(v'_9)$
7.623	0.68	$3p\sigma_y$	–	–	–	–
7.675 (s)	–	$3p\sigma_y + 1v_9$	–	–	–	0.052
7.725 (d)	–	$3p\sigma_y + 1v_8$	–	–	0.102	–
7.764 (s)	–	$3p\sigma_y + 1v_6$	–	0.141	–	–
7.798 (s)	–	$3p\sigma_y + 1v_4$	0.175	–	–	–
7.971	–	$3p\sigma_y + 2v_4$	0.173	–	–	–
8.149	–	$3p\sigma_y + 3v_4$	0.178	–	–	–
8.274	–	$3p\sigma_y + 3v_4 + 1v_6$	–	0.125	–	–
8.936	0.67	$4p\sigma_y$	–	–	–	–
9.053 (s)	–	$4p\sigma_y + 1v_6$	–	0.117	–	–
9.110	–	$4p\sigma_y + 1v_4$	0.174	–	–	–
9.158 (?)	–	$4p\sigma_y + 1v_6 + 1v_8$	–	–	0.105	–
9.177	–	$4p\sigma_y + 2v_6$	–	0.124	–	–
9.259	–	$4p\sigma_y + 1v_6 + 2v_8$	–	–	0.101	–
9.298	–	$4p\sigma_y + 3v_6$	–	0.121	–	–
9.425	–	$4p\sigma_y + 4v_6$	–	0.127	–	–
9.443	0.65	$5p\sigma_y$	–	–	–	–
9.556 (s)	–	$4p\sigma_y + 5v_6$	–	0.131	–	–
9.673 (s)	0.72	$6p\sigma_y$	–	–	–	–
9.821 (s)	0.67	$7p\sigma_y$	–	–	–	–
9.903 (b)	0.73	$8p\sigma_y$	–	–	–	–
9.963 (s)	0.63	$9p\sigma_y$	–	–	–	–

(s) means shoulder; (d) means diffuse structure; (?) assignment within bracket means uncertainty; (b) means broad structure.

Table 5
Energy values, quantum defect and assignment of the vibrational excitation $np\pi$ (carbon) Rydberg series converging to the ionic electronic ground state $\widetilde{X}^2A''(2a''^{-1})$ of C_2H_3Cl (energies in eV)

Energy	Quantum defect	Assignment	$\Delta E(v'_4)$	$\Delta E(v'_6)$	$\Delta E(v'_8)$	$\Delta E(v'_9)$
7.815	0.59	$3p\pi$	–	–	–	–
7.865	–	$3p\pi + 1v_9$	–	–	–	0.050
7.917	–	$3p\pi + 1v_8/2v_9$	–	–	0.102	0.052
7.945	–	$3p\pi + 1v_6$	–	0.130	–	–
7.971	–	$3p\pi + 3v_9$	–	–	–	0.054
7.981	–	$3p\pi + 1v_9 + 1v_6$	–	0.116	–	–
7.994	–	$3p\pi + 1v_4$	0.179	–	–	–
8.020	–	$3p\pi + 2v_8/4v_9$	–	–	0.103	0.049
8.046	–	$3p\pi + 1v_8/2v_9 + 1v_6$	–	0.129	–	–
8.072	–	$3p\pi + 5v_9/2v_6$	–	0.127	–	0.052
8.098	–	$3p\pi + 1v_8/2v_9 + 1v_6 + 1v_9$	–	–	–	0.052
8.125	–	$3p\pi + 3v_8$	–	–	0.105	–
8.170	–	$3p\pi + 2v_4$	0.176	–	–	–
8.200 (d)	–	$3p\pi + 3v_6$	–	0.128	–	–
8.235 (d)	–	$3p\pi + 4v_8$	–	–	0.110	–
8.988	0.59	$4p\pi$	–	–	–	–
9.093 (s)	–	$4p\pi + 1v_8$	–	–	0.105	–
9.130	–	$4p\pi + 1v_6$	–	0.142	–	–
9.232	–	$4p\pi + 1v_6 + 1v_8$	–	–	0.102	–
9.464 (s)	0.58	$5p\pi$	–	–	–	–
9.698 (s)	0.57	$6p\pi$	–	–	–	–
9.797	–	$6p\pi + 1v_8$	–	–	0.099	–
9.832	0.56	$7p\pi$	–	–	–	–
9.918	0.50	$8p\pi$	–	–	–	–

(d) means diffuse structure; (s) means shoulder.

promotion of an electron from a $p_{\|}$ to a Rydberg 6np orbital and is in good agreement with the 9.361 eV value reported by Locht et al. [6]. The *n*d series starting at 10.011 eV (Table 12), with a quantum defect $\delta = 0.11$ is also in good agreement with the value of 9.997 eV reported by Sze et al. [5]. The feature at 10.725 eV is quite intense and might also overlap with some other term of a higher series, therefore an alternative assignment is proposed below.

Table 6
Energy values, quantum defect and assignment of the vibrational excitation ndσ (carbon) Rydberg series converging to the ionic electronic ground state $\widetilde{X}^2A''(2a''^{-1})$ of C_2H_3Cl (energies in eV)

Energy	Quantum defect	Assignment	$\Delta E(v'_4)$	$\Delta E(v'_6)$	$\Delta E(v'_8)$	$\Delta E(v'_9)$
8.324	0.28	3dσ	–	–	–	–
8.377	–	$3d\sigma + 1\nu_9$	–	–	–	0.053
8.429	–	$3d\sigma + 2\nu_9/1\nu_8$	–	–	0.105	0.052
8.452 (s)	–	$3d\sigma + 1\nu_6$	–	0.128	–	–
8.478	–	$3d\sigma + 3\nu_9$	–	–	–	0.049
8.498	–	$3d\sigma + 1\nu_4$	0.174	–	–	–
8.512	–	$3d\sigma + 1\nu_6 + 1\nu_9$	–	–	–	0.060
8.530 (s)	–	$3d\sigma + 4\nu_9/2\nu_8$	–	–	0.101	0.052
8.560	–	$3d\sigma + 1\nu_6 + 2\nu_9$	–	–	–	0.048
8.574	–	$3d\sigma + 2\nu_6$	–	0.122	–	–
8.631	–	$3d\sigma + 3\nu_8$	–	–	0.101	–
8.646	–	$3d\sigma + 4\nu_9/2\nu_8 + 1\nu_6$	–	0.116	–	–
8.667	–	$3d\sigma + 2\nu_4$	0.169	–	–	–
8.676	–	$3d\sigma + 3\nu_8 + 1\nu_9$	–	–	–	0.045
8.728	–	$3d\sigma + 4\nu_8$	–	–	0.097	–
9.177	0.28	4dσ	–	–	–	–
9.559 (s)	0.24	5dσ	–	–	–	–
9.755	0.21	6dσ	–	–	–	–
9.852	0.36	7dσ	–	–	–	–
9.938	0.17	8dσ	–	–	–	–

(s) means shoulder; (?) assignment with in bracket means uncertainty (see discussion in text).

Table 7
Energy values, quantum defect and assignment of the vibrational excitation ndπ (carbon) Rydberg series converging to the ionic electronic ground state $\widetilde{X}^2A''(2a''^{-1})$ of C_2H_3Cl (energies in eV)

Energy	Quantum defect	Assignment	$\Delta E(v'_4)$	$\Delta E(v'_6)$	$\Delta E(v'_8)$	$\Delta E(v'_9)$
8.601	0.05	3dπ	–	–	–	–
9.284	0.06	4dπ	–	–	–	
9.386 (s)	–	$4d\pi + 1\nu_8$	–	–	0.102	–
9.400	–	$4d\pi + 1\nu_6$	–	0.116	–	–
9.490	–	$4d\pi + 2\nu_8$	–	–	0.104	–
9.541	–	$4d\pi + 2\nu_6$	–	0.141	–	–
9.596 (s)	–	$4d\pi + 3\nu_8$	–	–	0.106	–
9.600 (s)	0.07	5dπ	–	–	–	–
9.645	–	$5d\pi + 1\nu_9$	–	–	–	0.045
9.664	–	$4d\pi + 3\nu_6$	–	0.123	–	–
9.770	0.09	6dπ	–	–	–	–
9.871	0.14	7dπ	–	–	–	–
10.043 (s)	–	$7d\pi + 1\nu_4$	0.172	–	–	–

(s) means shoulder.

3.3.3. Rydberg series converging to the ionic electronic second excited state, $\widetilde{B}^2A''(1a''^{-1})$

Two series have been assigned to converge to the ionic energy 13.10 eV (Tables 13 and 14, Fig. 4) and attributed to the chlorine atom (Table 2). The energy position for the first member of each series, ns and np, lying at 9.541 and 10.543 eV corresponds to quantum defects $\delta = 2.05$ and 1.69, respectively. The former series has a slightly higher quantum defect for an ns Rydberg series, which might be due to the broad nature of the observed structure which may also be assigned to vibrationic excitations lying at the same energy (Table 13). These series have also been reported by Sze et al. [5] to lie at 9.997 and 10.513 eV close to the values reported in the present work.

Due to the intense nature of the feature observed at 10.725 eV for the previous Rydberg series converging to the ionic electronic first excited state, there may also be a contribution from the first member of a np series with a quantum defect of 1.59 converging to the ionic electronic second excited state might also be responsible for that.

3.3.4. Rydberg series converging to the ionic electronic third excited state, $\widetilde{C}(6a'^{-1})$

Only one feature has been assigned as converging to the third excited ionic state, $\widetilde{C}(6a'^{-1})$ this lies at 10.276 eV (Table 15) in close agreement with the value reported by Brion et al. [5] at 10.235 eV. This peak is assigned to the $n = 4$ member of a ns Rydberg series with a quantum defect $\delta = 1.98$, and appears to be associated with the chlorine atom.

Table 8
Energy values, quantum defect and assignment of the vibrational excitation *n*s (chlorine) Rydberg series converging to the ionic electronic first excited state $\tilde{A}^2A'(7a'^{-1})$ of C_2H_3Cl (energies in eV)

Energy	Quantum defect	Assignment	$\Delta E(v'_4)$	$\Delta E(v'_6)$	$\Delta E(v'_8)$	$\Delta E(v'_9)$
8.324	1.98	4s	–	–	–	–
8.377	–	$4s + 1v_9$	–	–	–	0.053
8.429	–	$4s + 2v_9/1v_8$	–	–	0.105	0.052
8.452 (s)	–	$4s + 1v_6$	–	0.128	–	–
8.478	–	$4s + 3v_9$	–	–	–	0.049
8.498	–	$4s + 1v_4$	0.174	–	–	–
8.512	–	$4s + 1v_6 + 1v_9$	–	–	–	0.060
8.530 (s)	–	$4s + 4v_9/2v_8$	–	–	0.101	0.052
8.560	–	$4s + 1v_6 + 2v_9$	–	–	–	0.048
8.574	–	$4s + 2v_6$	–	0.122	–	–
8.631	–	$4s + 3v_8$	–	–	0.101	–
8.646	–	$4s + 4v_9/2v_8 + 1v_6$	–	0.116	–	–
8.667	–	$4s + 2v_4$	0.169	–	–	–
8.676 (s)	–	$4s + 3v_8 + 1v_9$	–	–	–	0.045
8.728	–	$4s + 4v_8$	–	–	0.097	–
10.154	1.97	5s	–	–	–	–
10.157 (s)	–	$5s + 1v_8$	–	–	0.090	–
10.354	–	$5s + 2v_8$	–	–	0.107	–

(s) means shoulder.

Table 9
Energy values, quantum defect and assignment of the vibrational excitation *n*s (carbon) Rydberg series converging to the ionic electronic first excited state $\tilde{A}^2A'(7a'^{-1})$ of C_2H_3Cl (energies in eV)

Energy	Quantum defect	Assignment	$\Delta E(v'_4)$	$\Delta E(v'_6)$	$\Delta E(v'_8)$	$\Delta E(v'_9)$
8.498	0.92	3s	–	–	–	–
10.213	0.91	4s	–	–	–	–
10.311 (s)	–	$4s + 1v_8$	–	–	0.098	–
10.419	–	$4s + 2v_8$	–	–	0.108	–
10.472 (s)	–	$4s + 2v_8 + 1v_9$	–	–	–	0.053

(s) means shoulder.

Table 10
Energy values, quantum defect and assignment of the vibrational excitation *n*pπ (chlorine) Rydberg series converging to the ionic electronic first excited state $\tilde{A}^2A'(7a'^{-1})$ of C_2H_3Cl (energies in eV)

Energy	Quantum defect	Assignment	$\Delta E(v'_4)$	$\Delta E(v'_6)$	$\Delta E(v'_8)$	$\Delta E(v'_9)$
8.601	1.88	4pπ	–	–	–	–
8.710 (s)	–	$4p\pi + 1v_8$	–	–	0.109	–
8.775	–	$4p\pi + 1v_4$	0.174	–	–	–
8.834	–	$4p\pi + 1v_4 + 1v_9$	–	–	–	0.059
10.276	1.84	5pπ	–	–	–	–

(s) means shoulder.

Table 11
Energy values, quantum defect and assignment of the vibrational excitation *n*pπ (carbon) Rydberg series converging to the ionic electronic first excited state $\tilde{A}^2A'(7a'^{-1})$ of C_2H_3Cl (energies in eV)

Energy	Quantum defect	Assignment	$\Delta E(v'_4)$	$\Delta E(v'_6)$	$\Delta E(v'_8)$	$\Delta E(v'_9)$
9.354	0.56	3pπ	–	–	–	–
9.475	–	$3p\pi + 1v_6$	–	0.121	–	–
9.574	–	$3p\pi + 1v_6 + 1v_8$	–	–	0.099	–
10.503	0.54	4pπ				
10.629 (s)	–	$4p\pi + 1v_6$	–	0.126	–	–
10.675	–	$4p\pi + 1v_4$	0.172	–	–	–
10.763 (s)		$4p\pi + 2v_6$	–	0.134	–	–

(s) means shoulder.

Table 12
Energy values, quantum defect and assignment of the vibrational excitation *n*d (carbon) Rydberg series converging to the ionic electronic first excited state $\widetilde{A}^2A'(7a'^{-1})$ of C_2H_3Cl (energies in eV)

Energy	Quantum defect	Assignment	$\Delta E(v'_4)$	$\Delta E(v'_6)$	$\Delta E(v'_8)$	$\Delta E(v'_9)$
10.011	0.11	3d	–	–	–	–
10.117	–	$3d + 1v_8$	–	–	0.106	–
10.167 (s)	–	$3d + 1v_8 + 1v_9$	–	–	–	0.050
10.725	0.14	4d	–	–	–	–

(s) means shoulder.

Table 13
Energy values, quantum defect and assignment of the vibrational excitation *n*s (chlorine) Rydberg series converging to the ionic electronic second excited state $\widetilde{B}^2A''(1a''^{-1})$ of C_2H_3Cl (energies in eV)

Energy	Quantum defect	Assignment	$\Delta E(v'_4)$	$\Delta E(v'_6)$	$\Delta E(v'_8)$	$\Delta E(v'_9)$
9.541	2.05	4s	–	–	–	–
9.717	–	$4s + 1v_4$	0.176	–	–	–
9.887	–	$4s + 2v_4$	0.170	–	–	–
10.060	–	$4s + 3v_4$	0.173	–	–	–

Table 14
Energy values, quantum defect and assignment of the vibrational excitation *n*p (chlorine) Rydberg series converging to the ionic electronic second excited state $\widetilde{B}^2A''(1a''^{-1})$ of C_2H_3Cl (energies in eV)

Energy	Quantum defect	Assignment	$\Delta E(v'_4)$	$\Delta E(v'_6)$	$\Delta E(v'_8)$	$\Delta E(v'_9)$
10.543	1.69	4p	–	–	–	–
10.597	–	$4p + 1v_9$	–	–	–	0.054

Table 15
Energy values, quantum defect and assignment of the *n*s (chlorine) Rydberg series converging to the ionic electronic third excited state $\widetilde{C}(6a'^{-1})$ of C_2H_3Cl (energies in eV)

Energy	Quantum defect	Assignment
10.276	1.98	4s

3.4. Vibrational excitation coupled with the Rydberg series

Vibrational excitations associated with several of the Rydberg series are presented in detail in Tables 3–14. However, in order to avoid congestion in the Rydberg series, we have not labelled them in the figures. The four modes being excited are mainly those already reported for the valence excitation in the 6.0–7.5 eV energy region: they correspond to $v_4(a')$ excitation C=C stretching, $v_6(a')$ H–C–Cl scissoring, $v_8(a')$ C–Cl symmetric stretching and $v_9(a')$ CH_2 in plane rocking. The excitation of these modes is characterized by energies of 0.170, 0.125, 0.100 and 0.050 eV. These values are in good agreement to those reported by Locht et al. [6].

A close analysis of the data reveals in some cases what seems to be the activation of two different modes. In fact, we have already noticed that the normal mode description of vibrations is very powerful for the lowest lying excitations, with the possibility of strong Fermi resonances throughout the vibronic assignments. An example of this is the peak at 7.917 eV, where we assign it as $3p\pi + 1v_8/2v_9$ since we are not able to distinguish in between $1v_8$ and $2v_9$.

4. Absolute photo-absorption cross-sections

Using the Beer–Lambert law (see Section 2) we have derived absolute photo-absorption cross-sections over the range $300 > \lambda > 115$ nm (6.1–10.8 eV). Since we have measured absolute photo-absorption cross section for more than 50 compounds and validated our measurements against known benchmarks, we believe that our data provide the most accurate values to date. The present cross-section values are quite different from those reported in earlier data [4]. The $\pi \rightarrow \pi^*$ band is determined to have a maximum cross section of 31.460 Mb at 6.709 eV almost three times higher than the photo-absorption data of Sood and Watanabe [4].

Using these cross-section values the atmospheric destruction of C_2H_3Cl by UV photolysis was modelled as a function of altitude using a program previously described by Limão-Vieira et al. [11]. Photolysis rates at a given wavelength were calculated as the product of the Solar Actinic Flux [12] and the molecular photo-absorption cross-section at 1 km altitude steps from the surface up to the stratopause (50 km). At each altitude a total photolysis rate may then be calculated by summing over the individual photolysis rates for that altitude. The reciprocal of the total photolysis rate for a given altitude gives the local photolysis lifetime at that altitude, i.e. the time taken for the molecule to photo-dissociate at the altitude assuming that the solar flux remains constant. These results reveal that the photolysis lifetime of vinyl chloride varies from several years near the ground to just over one day at

30 km. Therefore, the present results suggest that photolysis by solar UV radiation may play a significant role in the destruction of vinyl chloride in the high stratosphere.

5. Conclusions

We have measured high resolution VUV spectra over the energy range between 5.0 and 10.8 eV of vinyl chloride using synchrotron radiation as the irradiating light source. Photo-absorption bands belonging to valence transitions and Rydberg transitions are observed in the spectra. All of these bands have been identified, with several new structures being observed and assigned for the first time. The absolute photo-absorption cross-section is reported and used to derive photolysis rates for vinyl chloride in the terrestrial atmosphere from the surface to the stratosphere.

Acknowledgements

We are pleased to acknowledge the support of the I3 project IA-SFS, contract number RII3-CT-2004-506008 for the use of the ISA facilities at University of Aarhus, Denmark. We also thank the EU EPIC network HPRN-C-2002-00179 and the EPSRC for financial support. Eva Vasekova thanks the Open University for the support of a postgraduate studentship. P.L.V. acknowledges the visiting fellowship position at The Open University, UK.

References

[1] I. Rozum, P. Limão-Vieira, S. Eden, J. Tennyson, N.J. Mason, J. Phys. Chem. Ref. Data 35 (2006) 267.
[2] N.J. Mason, A. Dawes, R. Mukerji, E.A. Drage, E. Vasekova, S.M. Webb, P. Limão-Vieira, J. Phys. B 38 (2005) S893.
[3] A.D. Walsh, Trans. Faraday Soc. 41 (1945) 35.
[4] S.P. Sood, K. Watanabe, J. Chem. Phys. 45 (1966) 2913.
[5] K.H. Sze, C.E. Brion, A. Katrib, B. El-Issa, Chem. Phys. 137 (1989) 369.
[6] R. Locht, B. Leyh, K. Hottmann, K.H. Baumgartel, Chem. Phys. 220 (1997) 207.
[7] S. Arulmozhiraja, R. Fukuda, M. Ehara, H. Nakatsuji, J. Chem. Phys. 124 (2006) 034312.
[8] S. Eden, P. Limão-Vieira, S.V. Hoffmann, N.J. Mason, Chem. Phys. 323 (2006) 313.
[9] G. Herzberg, Molecular Spectra and Molecular Structure, III. Electronic Spectra and Electronic Structure of Polyatomic Molecules, Van Nostrand, New York, 1966.
[10] M.B. Robin (Ed.), Higher Excited States of Polyatomic Molecules, vol. II, Academic Press, New York, 1975.
[11] P. Limão-Vieira, S. Eden, P.A. Kendall, N.J. Mason, S.V. Hoffmann, Chem. Phys. Lett. 364 (2002) 535.
[12] Chemical kinetics and photochemical data for use in stratospheric modeling, Evaluation number 12, NASA, Jet Propulsion Laboratory, JPL Publication 97-4, January 15, 1997.